AIP | Review of Scientific Instruments

A long path length pulsed slit valve appropriate for high temperature operation: Infrared spectroscopy of jet-cooled large water clusters and nucleotide bases

Kun Liu, Raymond S. Fellers, Mark R. Viant, Ryan P. McLaughlin, Mac G. Brown, and Richard J. Saykally

Citation: Review of Scientific Instruments **67**, 410 (1996); doi: 10.1063/1.1146605
View online: http://dx.doi.org/10.1063/1.1146605
View Table of Contents: http://scitation.aip.org/content/aip/journal/rsi/67/2?ver=pdfcov
Published by the AIP Publishing

A long path length pulsed slit valve appropriate for high temperature operation: Infrared spectroscopy of jet-cooled large water clusters and nucleotide bases

Kun Liu, Raymond S. Fellers, Mark R. Viant, Ryan P. McLaughlin, Mac G. Brown, and Richard J. Saykally
Department of Chemistry, University of California, Berkeley, California 94720

(Received 20 September 1995; accepted for publication 28 November 1995)

We report the design and performance of a pulsed slit valve for generation of supersonically cooled species in a long path length planar expansion. Utilizing three commercial solenoids driven synchronously by an economic power transistor circuit, the valve produces pulses adjustable in width from 500 to 1000 μs with a repetition rate up to 80 Hz. The pulsed valve can be operated continuously for 12 h, and operation over one month is typical before major maintenance is required. The path length $\times$ density product attained by this pulsed source is sufficient for observing large cluster species, such as the water hexamer, on our far-infrared spectrometer. With the addition of a detachable sample oven, it can also be heated up to 230 °C to inject nonvolatile molecules into planar supersonic expansions. © *1996 American Institute of Physics.* [S0034-6748(96)05602-4]

I. INTRODUCTION

The development of supersonic free jets has had a tremendous impact on chemical physics.[1,2] Two particular subjects for which our understanding has been greatly enhanced by this advance are weakly bound clusters[3] and biological molecules.[4] In the former context, the subsequent development of both cw[5] and pulsed[6] slit jet expansions enabled detailed studies of many weakly bound dimers, and a small number of trimers, tetramers, and pentamers, by mid-IR[7] and far-IR[8] laser spectroscopy. A number of reviews on the design of such sources[9,10] and on the physics of clustering in supersonic expansions[11–13] have been published.

Pulsed slit jets are of particular relevance as one seeks to address sequentially larger cluster systems by laser absorption spectroscopy, for several reasons. First, a pulsed jet can offer higher instantaneous beam intensities, and consequently larger clusters, than a cw jet expanded through a nozzle of the same geometry, while also reducing the gas load on the vacuum pumps as a result of the low duty cycle. Second, the spectral linewidth is reduced to below the room temperature Doppler limit by the high degree of collimation of the wedge-shaped supersonically expanding gas. Third, the path length $\times$ density product is much larger for a slit jet, as compared to a pinhole expansion. This is due both to the geometry and to the fact that the density drops as $1/D$ for a slit (D=distance from the nozzle) instead of $1/D^2$, as for a pinhole. This latter feature also enhances the production of larger clusters in the expanding jet.

Since the first successful implementation of a pulsed planar supersonic jet for high resolution spectroscopy by Amirav, Even, and Jortner,[14] who employed two spinning concentric cylinders with a slit length of 35 up to 90 mm, many slit valve designs have been demonstrated for the studies of weakly bound clusters. Among the variety of possible mechanical designs, the most convenient approach employs a solenoid actuated mechanism. Typical examples of this type are given by Lovejoy and Nesbitt,[6] and Sharpe *et al.*[15] Both designs have since been refined from their original versions. While in the former case, the maximum slit path length is now 40 mm[7] in the latter can be as long as 120 mm.[16] We note general similarities in design between the Berkeley room temperature slit valve described below and the one by Sharpe and co-workers from Pacific Northwest Laboratory.

Here we describe a slit valve design that is simple to construct, reliable to operate, and adapted to heating up to 230 °C in order to study nonvolatile systems, such as the nucleotide bases. Utilizing three synchronized commercially available solenoids, driving a 101.6 mm by 0.127 mm slit produces planar jets with a pulse width that is adjustable from a few hundred microseconds up to a millisecond. Continuous operation at an 80 Hz repetition rate for up to 12 h, and consecutively for up to weeks with minimal maintenance introduces no noticeable change in performance. Combined with a confocal optical multipass cell on the Berkeley tunable far-infrared laser spectrometers[17] and tunable diode laser spectrometer,[18] a total absorption path length of 22 (as many as 50 for the mid-IR experiment)$\times$101.6 mm can be readily achieved in the high density region of the planar supersonic expansion.

In our far-infrared vibration–rotation–tunneling spectroscopy (FIRVRTS) studies of water clusters, a substantial improvement (up to an order of magnitude) in the signal-to-noise (S/N) ratio has been accomplished for the absorptions observed previously with a continuous planar supersonic jet[5] of the same slit dimensions. Furthermore, it is found that large clusters, such as the water pentamer,[19] can only be observed with the pulsed planar jet under the same absorption limits on our spectrometer. In the tunable infrared diode laser experiments, this valve has not only been used at room temperature to generate water clusters, but also heated to $\sim$230 °C to obtain the jet-cooled absorption spectrum of the nonvolatile nucleotide base uracil.[20]

The rest of this paper is organized as follows. In Sec. II, a detailed mechanical construction of the valve is given, followed by the description of an electronic driver circuit for

 0034-6748/96/67(2)/410/7/$10.00

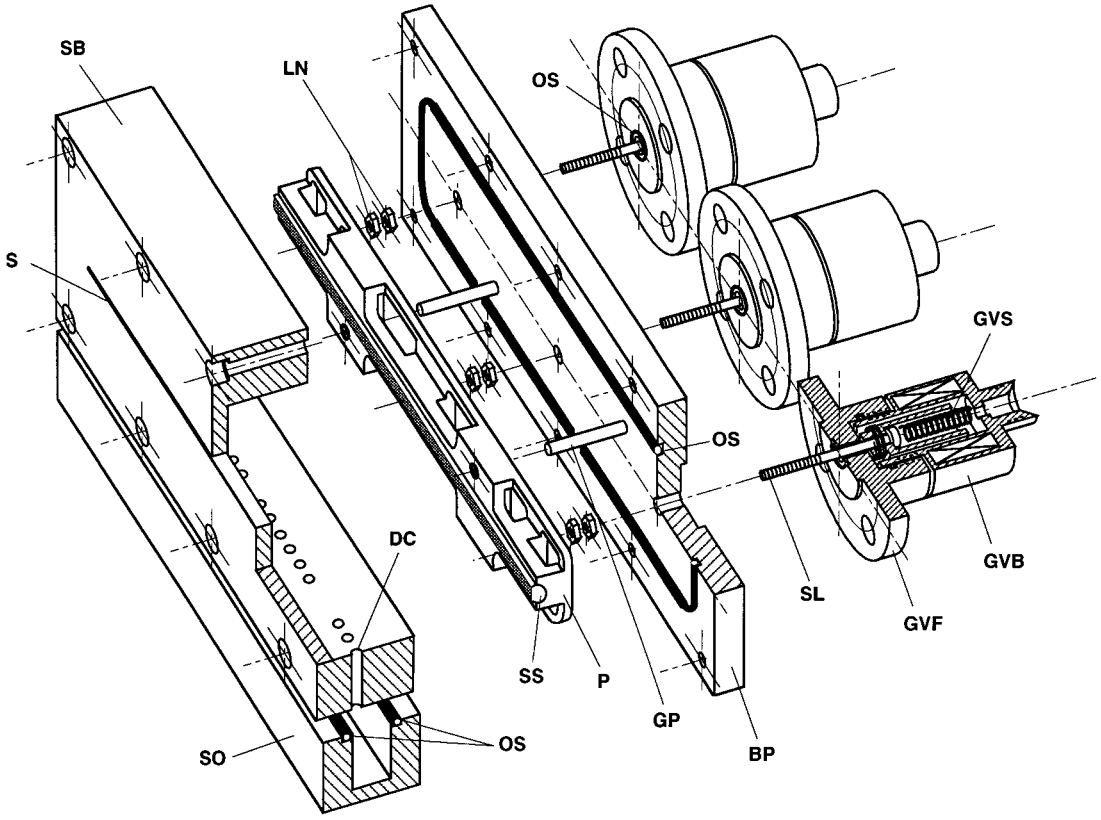

FIG. 1. The cutaway view of the valve: BP—backplate of the valve, DC—diffusion channel for the sample vapor to enter the slit body; GP—guiding post for restricting the poppet motion, GVB—commercial general valve (GV) solenoid body, GVF—solenoid mounting flange, GVS—compression spring inside the solenoid, LN—locking nuts to turn the screw links as well as to lock the screws in position, OS—O-ring seal, P—poppet, S—slit, SB—slit body, SL—screw linkage replacing the commercial poppet, SO—detachable sample oven, SS—slit sealing cord, the front surface of which is sanded flat.

three synchronous solenoids. Section III discusses the overall operation. Cluster number density and sensitivity estimates, together with the experimental data obtained using the valve, are presented in Sec. IV.

II. CONSTRUCTION

A. Mechanical design

1. Room temperature

The main body of the source is constructed from two stainless steel (300 series) parts, a removable front section (slit body), and a backplate on which the solenoid valves are mounted, as shown in Fig. 1. A Buna-N O-ring provides a vacuum seal between the separate sections. The inside of the slit body is milled to a depth of 12.7 mm to accommodate a poppet, which connects to the solenoid mechanism through a screw linkage. The slit body depth and thereby the screw linkage length were minimized so as to facilitate the agile response of the poppet to the moving plungers inside of the solenoids.

The slit, with dimensions of 101.6 mm by 0.127 mm, is located in the front face of the slit body. It was cut using electrical discharge machining (EDM), and has a throat length of 3.2 mm. A longer throat length of 4.8 mm has been found to yield weaker cluster signals due to the interfering turbulence layers established inside the nozzle; the thickness of the turbulence layer is determined by the ratio of the slit width to the throat length, for a given Reynold's number. The slit is sealed from the inside of the source body using a 105-mm-long, 2.77-mm-diam Buna cord, which is set in the front face of the poppet.

The poppet must be strong and light, and hence is constructed from aluminum. The Buna cord is trapped within a groove in the poppet, the cross section of which is best described as a partially buried semicircle. This was machined by drilling a hole along the length of the poppet and then milling off the front face until the hole was exposed as a channel. The width of this channel is only slightly smaller than the Buna cord such that the cord can be easily pushed into the groove without being stretched first. We found this procedure useful to avoid two unwelcome results; (a) a stretched O-ring takes a long time to relax to its original shape and thus changes the seal performance during operation, and (b) if a cord has to be stretched to fit in the groove, its exposed area will be too small for the flat sanding procedure described below. A light application of Krazy glue in the groove helps further secure the cord. To achieve a good seal of the Buna cord against the slit, two steps must be taken. First, the side of the Buna cord which contacts the slit is sandpapered (No. 600 sandpaper) flat, such that the Buna is only just proud of the front face of the poppet. Second, the

inside surface of the source body around the slit must be polished.

Two stainless steel guiding posts (12.7 mm long, 3.175 mm in diameter) mounted on the inside of the backplate, restrict the movement of the poppet to only the forward and backward direction. To facilitate a smooth motion, Teflon™ bushings are located within the holes in the poppet through which the guide posts extend. The height of the post is designed to be the same as the depth of the slit body; this serves as a guide for valve adjustment described latter.

Mounted on the outside of the backplate are three commercial solenoid valves (General Valve Corporation, series 9). Two modifications were made on the supplied mounting flange. A 12.7-mm-diam step on the front side of the flange was lathed to match the counter bore on the back of the mounting plate. This ensures the concentric alignment of the solenoid to the gas entrance channel on the backplate. The exit hole on the flange has been enlarged to increase gas throughput, as well as to decrease the tendency of frictional wearing between the screw link and the flange.

Three stainless steel screw links (4–40 threads) replace the commercial ''poppets'' (manufacturer's notation). These screws each need to be set at the correct length (~19 mm) to ensure that the poppet lies both parallel to and flush with the inside of the slit, resulting in a good seal when the solenoids are deactivated. To achieve this the screws should be tightened into the poppet; stainless steel helicoils are buried within the poppet to provide durable threads. With all the solenoid parts fully installed, the ends of the post guides should lie just below the front faces of the bushings. Once correctly located, each screw is locked in place using two nuts. The same locking nuts also provide the turning mechanism of the screws, which are specially machined to have a flat head so as not to distort the compression spring inside the plunger.

Three gas inlet lines enter the source, one attached to the back of each solenoid assembly. Incoming gas passes along these lines and through the central channels within the solenoids before entering the main source body. Only when the solenoids are activated and the poppet is retracted from the slit can a gas pulse escape.

Not shown in Fig. 1 are two strip angles for mounting the valve to any fixture. The angles are attached to the rear side of the backplate in between the solenoid mounting flanges. The appropriate sides of the round flanges were cut off on a sand grinder to yield space for the angles. In our configuration, the angles were then mounted on a translational stage for adjusting the downstream distance between the slit and the multipassing laser beam.

2. High temperature

The main body of the high temperature source has the same basic design as the room temperature version described above, but it also includes a detachable sample reservoir on the bottom for holding solids or liquids. It is constructed entirely from materials that can withstand high temperature operation. The main source body and sample reservoir are connected by an array of sample diffusion holes located just below the poppet. Heating is accomplished using two strip heaters (Omega, OT-715 150 W); one is attached to the top of the main source body and the other to the bottom of the sample reservoir. Type *J* thermocouples are used to monitor the temperature at various points on the slit body and the sample reservoir.

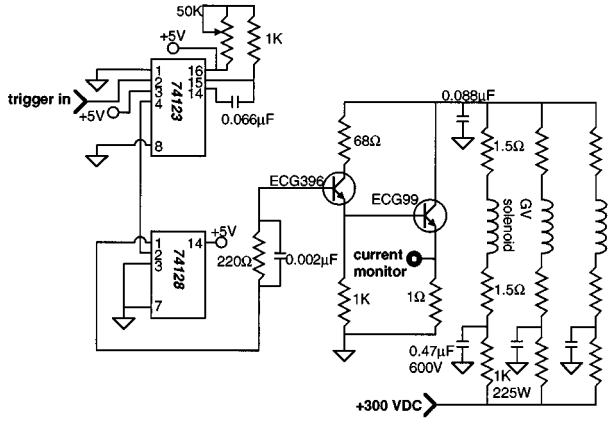

FIG. 2. Three channel solenoid driving circuit. The required external trigger can be supplied by a function or pulse generator. Under normal operating conditions, the three solenoids draw an average current of 70 mA from the regulated dc power supply. The transistor ECG99 can be replaced by a higher rating ECG98. To prevent inductive high voltage spikes from damaging the transistor, appropriate Zener diodes can be connected to the collector of ECG99.

Several modifications were required to adapt the room temperature valve for high temperature operation. The source is constructed from copper to ensure even heating, and is gold coated to minimize surface-initiated decomposition of the biological samples. The slit is sealed with a Viton cord. While the Viton generally works well, it tends to harden over time and has to be replaced after approximately 20 h of high temperature use. Vespel bushings are used instead of Teflon to help the poppet ride smoothly on the guide posts. The source is mounted between two 19.05-mm-diam stainless steel rods which are, in turn, attached to a vacuum chamber flange via pipe fittings (Cajon UltraTorr). Macor spacers placed between the rods and the source act as thermal insulators, keeping the source temperature stable. To prevent condensation of the sample vapor, the carrier gas is preheated by wrapping heating tape around the three stainless steel inlet tubes leading into the back of the solenoid valves. Fine copper wire placed inside of this tubing maximizes the hot surface area exposed to carrier gas, hence increasing the efficiency of the preheating.

The source can be operated at temperatures up to 230 °C, limited mainly by the integrity of the solenoid valves. Higher temperatures could be achieved by cooling the solenoids directly and using a more durable elastomer such as Kalrez instead of Viton.

B. Driving electronics

The synchronous operation of the three solenoids is accomplished with a fast power switching transistor circuit (Fig. 2). The circuit described here is by no means unique

but it is easy and economic to construct. It consists of two parts—timing and power switching.

An external trigger transistor–transistor logic (TTL) pulse is provided by either a function or pulse generator; only the rising edge of the pulse is necessary. The adjustable pulse width is determined by the RC time constant between pins 14 and 16 on the dual multivibrator (74123). A buffer invertor (74128) is used to protect the timing circuit from the transistor switching part. To achieve fast response, a speedup 0.002 μF capacitor[21] is connected across the 220 Ω base resistor.

Two high voltage switching transistors are utilized to ensure sufficient amplification of the low TTL current in order to activate the solenoids. For each solenoid channel, the voltage is applied by a KEPCO 400 VDC, 400 mA power supply through a ballast resistor (1 kΩ, 225 W) and a power capacitor (0.47 μF, 600 VDC). The total current profile can be monitored by measuring the voltage across a 1 Ω resistor at the emitter of transistor ECG99. Inductive voltage spikes from the solenoid can be prevented from damaging the transistor by using appropriately rated Zener diodes at the collector or a bypass diode and resistor[21] in parallel to each solenoid. Presently, only a capacitor is employed for this purpose.

III. OPERATION

Three solenoids are activated simultaneously by a single current pulse, the temporal profile of which is displayed in Fig. 3. Uncoordinated plunger motion leads to a distorted current wave form and an uneven gas pulse across the slit. If proper adjustment is achieved by rotating the solenoids, the resulting strong magnetic field will pull all three ferromagnetic plungers into the core of the solenoids. Through the screw linkage, the concerted plunger motion lifts the sealing poppet evenly away from the slit nozzle. The spring tension and the end of the plunger travel are adjustable simultaneously by turning the solenoid body, which is what primarily determines the temporal length of the gas pulse. The plunger can bounce back toward its rest position after it hits the bottom of the solenoid core. The holding current pulse length and amplitude need to be adjusted to minimize bouncing the plunger against the travel stop and the poppet against the nozzle. With the present circuit, the peak current monitored at the 1 Ω resistor is about 1600 mA and the optimal pulse width is between 500 and 700 μs. A longer gas pulse requires higher holding current, which can be achieved with a smaller ballast resistance.

The heated source operates in a similar fashion to the room temperature source except for a few changes due to high temperature running and the nature of the samples studied. During operation the hot sample vapor diffuses from the reservoir into the main source body. Here, the sample is mixed with the preheated carrier gas before expanding through the pulsed slit. The top heater is kept at a higher temperature than the lower heater to ensure that no condensation of the sample occurs in either the source body or the slit. The temperature stability of the source is affected by the gas flow rate. For a given repetition rate and stagnation pressure, a steady source temperature can be reached. The source can be operated at up to 80 Hz, but in practice, it is generally run at 35–40 Hz.

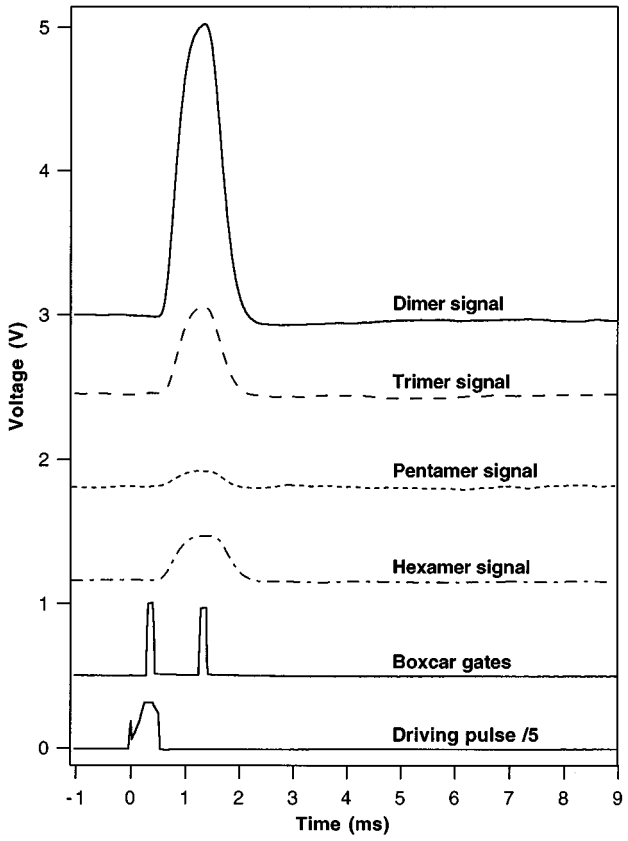

FIG. 3. Overlay of the important timing sequences during one trigger event on the FIRVRT experiment. Signals (acquired from a digital averaging scope) from different D_2O (except that the hexamer is of pure H_2O) clusters were taken at different laser absorption frequencies. The first boxcar gate samples the background of the signal trace, while the second samples the peak of the absorption profile. The subtraction of the two gated signals was performed on an analog processor (Stanford Research System), which in turn was displayed on a computer.

The solenoid resistance changes with increasing temperature, and this alters the tuning of the valves. Hence, while the room temperature source does not need adjustment during operation, the high temperature source needs to be optimized *in situ* after attaining the desired temperature. This adjustment is accomplished by slightly rotating the gas inlet tubes that connect to the back of each solenoid, until the background pressure in the vacuum is maximized, indicating the maximum throughput condition.

IV. PERFORMANCE

As a numerical example, we estimate the number densities of various water clusters produced and absorption detection limits attainable with the pulsed slit jet using the Beer–Lambert law. The number density drops as $1/\delta$, where δ ($=D/d$, d being the slit width of $\sim$0.102 mm) is a reduced center line downstream distance from the nozzle.[11] The nozzle stagnation temperature and pressure are 310 K (under normal operations the nozzle temperature is slightly higher than room temperature due to mechanical friction and undissipated heat from the solenoids) and 1.5 atm, respectively.

Roughly 1% of the water molecules seeded in a ~2% mixture is conservatively assumed to form dimers, while a factor of 5 sequential reduction for higher clusters is adopted in the following density calculations. Under these conditions, the center line number density of the water dimer is on the order of 10^{12}–10^{13} cm^{-3} at downstream distances ranging from 1 to 5 cm, where the multipassing laser intersects the pulsed jet. The corresponding hexamer density exceeds 10^9 clusters/cm^3. The thermal distribution over rotational states at 5 K leads to a 10- to 100-fold reduction of these number densities for each quantum state. Based on the absorbance sensitivity of $10^{-6}/(Hz)^{1/2}$ for the Berkeley far-infrared (FIR) spectrometers, [17] a typical path length of 224 cm, and a reasonable peak absorption cross section of 10^{-14} cm^2 per cluster species for a ~5 MHz linewidth, we estimate a detection limit on the order of 10^5 clusters /cm^3 per $Hz^{1/2}$ per quantum state. In a 10 kHz detection window arising from the time constant of the lock-in amplifier, this translates into a sensitivity of $\sim 10^7$ clusters/cm^3 per quantum state per pulse. Further improvements on this limit derive from the gated signal averaging, wherein more than an order of magnitude gain in S/N can be readily achieved. From the above estimate, it is clear that the sensitivity attained with the pulsed slit jet is more than adequate for observing intermediate size cluster species such as the water pentamer[19] and hexamer.[22]

Figure 3 displays a series of signal traces for VRT transitions in various size water clusters, together with the driving current pulse. The FIR absorption signal is recovered with a digital lock-in amplifier (Stanford Research Systems, SRS830) operating at 100 μs time constant and $2f$ detection, where f is the reference frequency for frequency modulation (FM) of the laser. The transient output of the lock-in is then fed into the boxcars (SRS250) for gated signal integration and averaging; one samples the peak of the transient absorption, and the other the background. Due to the detection scheme, the 900 μs full width at half-maximum (FWHM) signal pulse width does not represent the true gas pulse width. The former is an upper bound of the latter; a longer time constant further extends the signal pulse width. The 1.3 ms delay between the onset of the current pulse and the peak signal is also primarily due to the lock-in detection. A direct real-time observation of the signal with only a preamplifier after the detector indicates a 350 μs corresponding delay, which is a reasonable time for the plunger to lift the poppet away from the slit. As expected and noticed in Fig. 3, the absorption signals of different clusters occur at the same time relative to the triggering current pulse because of the similar center line translational temperature in the seeded jet. The velocity slip effect viz. the phenomenon of different species traveling at different mean velocities in the supersonic coexpansion of mixed gases, cannot be observed with the temporal resolution of our experiments. The signals are observed with a total optical path length of 223.5 cm achieved by a confocal multipass cell; the long axis waist of the elliptical multipass pattern is 4 cm, and is located with one edge 1 cm downstream of the nozzle. Water clusters are produced by bubbling Ar at 1.5 atm through room temperature water and expanding the saturated vapor through the slit nozzle. A 1345 ℓ s^{-1} mechanical booster (Edwards), backed by two rotary pumps (Edwards, model E2M275), is used to handle the high gas throughput of the nozzle. While in general the absorption signal was observed at a background pressure of 25 mTorr with Ar carrier gas (higher for lighter gases such as Ne and He) at a repetition rate ranging from 40 to 60 Hz, slightly different optimal conditions were found for different size water clusters. Water dimer and trimer prefer higher backing (1.8 atm) and background (30 mTorr) pressures than the larger clusters such as the hexamer, for which the corresponding values are 1.5 atm and 25 mTorr, respectively; sensitive to these small differences in pressures, the signal intensity can change by up to a factor of 3. Arguably, the difference in the cluster formation kinetics is primarily responsible for the above observations; e.g., lower backing pressure leads to an effective increase in the water vapor concentration, preferentially producing larger clusters. A 1200 sccm mass flow rate was measured under the above operating conditions.

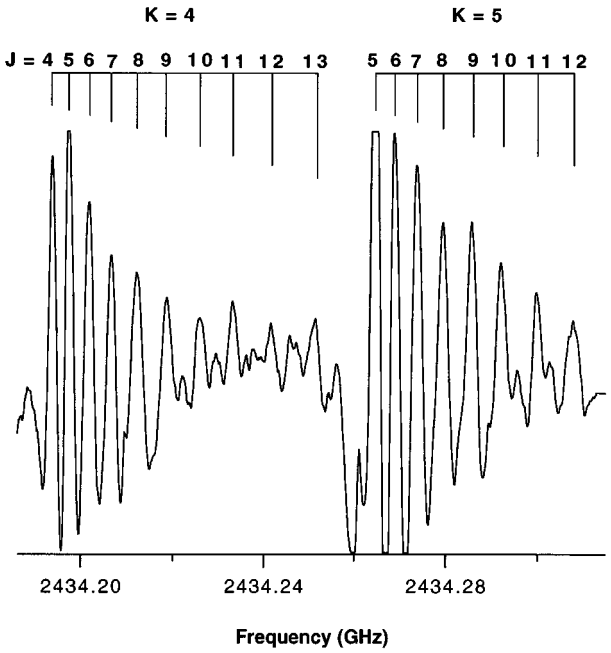

FIG. 4. A portion of the Q branch of the cyclic water pentamer $(D_2O)_5$ VRT spectrum. Rotational quantum numbers J and K are labeled. The flattop in the plot was due to the off-scale signal. The high S/N (better than 50:1 has been obtained for stronger transitions not shown here) indicates efficient production of this large cluster by the pulsed slit valve; no pentamer absorption has been observed previously with a cw slit of the same dimensions on our spectrometer. A careful simulation (including both Hönl–London and Boltzmann factors) of the relative intensities of all the Q branch lines yields a rotational temperature of 5–6 K.

Significant improvements in sensitivity of the FIR spectrometers have been made by incorporating the pulsed slit source, relative to the cw source of the same geometry.[5] Figure 4 shows a portion of the Q branch region in the FIRVRT spectrum of the water pentamer,[19] which has not been observed with the cw source. Compared with the cw nozzle, the apparent disadvantage of the low duty cycle in the pulsed source has been compensated for by a much more intense pulsed jet containing higher concentrations of larger clusters. The 5 MHz linewidth observed when a transition is fully

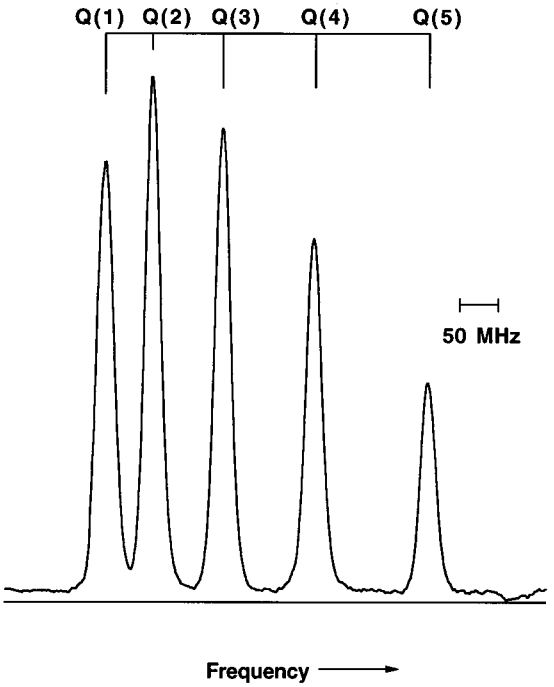

FIG. 5. A spectrum of the Q branch region of the single ^{15}N substituted N_2O obtained on the Berkeley mid-IR tunable diode laser spectrometer under heated source conditions. The supersonic jet was prepared with a 1% N_2O seeded in He at a stagnation pressure of 2.5 atm. Rotational quantum number J is labeled in the parentheses. A rotational temperature of 8.0 ± 0.5 K results from fitting the relative intensities of $Q(1)$ through $Q(5)$ to a Boltzmann distribution for the linear N_2O. Heating the source to 220 °C did not create any discernible line broadening.

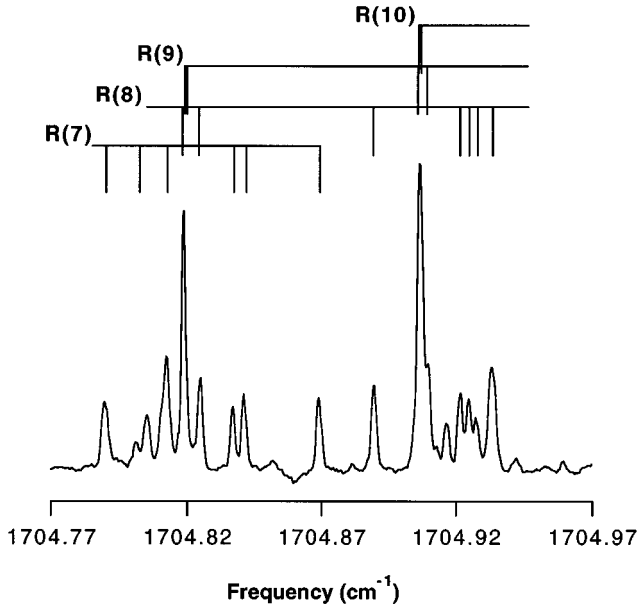

FIG. 6. A 0.2 cm^{-1} region of the ν_6 vibrational band of jet-cooled uracil, with spectroscopic assignments labeled as $R(J)$ [each thick mark represents different K_a and K_c quantum numbers in a given $R(J)$ manifold], using the heated pulsed slit valve on the diode laser spectrometer. The experimental conditions are described in the text. At 210 °C, the vapor pressure of uracil is 75 mTorr. The rotational temperature is difficult to estimate due to the unreliable determination of relative signal intensities; however, we estimate 20 K as an upper limit.

modulated is the same as that obtained in a continuous jet. It is mainly determined by the nonorthogonal intersection of the laser beam and the supersonic jet due to the multipass geometry; attempts to skim the planar expansion did not further reduce the linewidth. The Doppler width estimated for passing a single laser beam parallel to the slit should be slightly narrower. The observed overall spectrum is consistent with a rotational temperature of 5–6 K in an intensity simulation considering both the Boltzmann and Hönl–London factors, which is about the same value as observed for the cw planar jet.[5] This rotational temperature has also been confirmed in other clusters such as $(D_2O)_3$ and $(H_2O)_3$.[23,24] An order-of-magnitude increase in S/N has been observed on the signals of the tetramer[25] and trimer,[24] which were previously studied in a cw slit jet. In addition, strong signals from an exotic isotopically substituted trimer $(D_2O)_2HOD$ have been first observed with the pulsed jet by bubbling Ar through 99.9% D_2O at room temperature, even though previously the same spectral region had been carefully scanned with a cw slit jet.[26] Note that the probability of forming this mixed trimer relative to that of $(D_2O)_3$ is only 1:999 in the jet.

We also tested the source performance on our mid-IR tunable diode laser spectrometer. The apparatus is similar to that described elsewhere.[18] Briefly, the transient absorption signal from the IR detector is amplified, bandpass filtered (3–30 kHz), and acquired by two gated boxcar integrators. A total path length of 4.0 m was accomplished again using a confocal multipass cell together with the slit nozzle.

To characterize supersonic cooling under heated source conditions, we probed the Q branch portion of the $01^10 \leftarrow 00^00$ $^{15}N^{14}N^{16}O$ rovibrational band at 585.3 cm^{-1} (Figure 5). The ^{15}N isotope (0.7% natural abundance) was chosen to reduce the interfering $^{14}N_2O$ absorption in the background of the vacuum chamber. At a source temperature of 200–220 °C, a stagnation pressure of 2.5 atm He (containing ~1% nitrous oxide), and a repetition rate of 35 Hz with a solenoid current pulse width of ~500 μs, the intensity distribution of the Q branch agrees well with a Boltzmann rotational temperature of 8.0 ± 0.5 K. A recording of the same spectrum under similar conditions, except holding the source at room temperature, yielded a corresponding temperature of 4.0 ± 0.5 K. A higher repetition rate and longer pulse width tended to cause fluctuations of the source temperature greater than 5 °C. The observed 0.001 cm^{-1} (30 MHz) FWHM of the peaks was primarily due to the instability of the laser frequency and not due to Doppler broadening. Furthermore, there was no discernible broadening of the peaks upon heating the source.

To initiate our effort to study hydrogen-bonded clusters containing DNA and RNA bases, we have used the heated slit valve to generate jet-cooled uracil. Operating at a temperature of 190 °C for the sample reservoir and 210 °C for the slit body, while maintaining other conditions similar to those in the N_2O experiment, we observed the ν_6 fundamental band (a-type mixed carbonyl stretching vibration) of uracil, centered around 1703.888 cm^{-1}.[20] Figure 6 shows a 0.2 cm^{-1} region of the R branch, including rotational quantum number assignments. The pure rotational spectrum of

uracil was first reported by Brown *et al.* using a microwave spectrometer and heated cw pinhole supersonic jet.[27] That work measured 65 pure rotational transitions with a typical S/N of 10:1. Comparing the S/N ratios obtained in the two different experiments, and also considering the fact that microwave spectrometers are typically 10–100 times more sensitive than mid-IR diode laser spectrometers, the advantage of the large path length × density product afforded by the pulsed slit is clearly evident.

ACKNOWLEDGMENTS

M.R.V. thanks the Royal Commission for the Exhibition of 1851 for a postdoctoral research fellowship. This work was supported by the Experimental Physical Chemistry Program of the National Science Foundation (Grant No. CHE-9424482).

[1] R. E. Smalley, L. Wharton, and D. H. Levy, Acc. Chem. Res. **10**, 139 (1977).
[2] R. Campargue, J. Phys. Chem. **88**, 4466 (1984).
[3] K. R. Leopold, G. T. Fraser, S. E. Novick, and W. Klemperer, Chem. Rev. **94**, 1807 (1994).
[4] T. R. Rizzo, Y. D. Park, and D. H. Levy, J. Am. Chem. Soc. **107**, 277 (1985).
[5] K. L. Busarow, R. C. Cohen, G. A. Blake, K. B. Laughlin, Y. T. Lee, and R. J. Saykally, J. Chem. Phys. **90**, 3937 (1989).
[6] C. M. Lovejoy and D. J. Nesbitt, Rev. Sci. Instrum. **58**, 807 (1987).
[7] D. J. Nesbitt, Ann. Rev. Phys. Chem. **45**, 367 (1994).
[8] R. J. Saykally and G. A. Blake, Science **259**, 1570 (1993).
[9] W. R. Gentry, in *Atomic and Molecular Beam Methods*, edited by G. Scoles (Oxford University Press, New York, 1988), Vol. I, pp. 54–82.
[10] M. Kappes and S. Leutwyler, in Ref. 9, pp. 380–415.
[11] O. F. Hagena, Surf. Sci. **106**, 101 (1981).
[12] S. B. Rayli and J. B. Fenn, Ber. Bunsenges. Phys. Chem. **88**, 245 (1984).
[13] G. D. Stein, Surf. Sci. **156**, 44 (1985).
[14] A. Amirav, U. Even, and J. Jortner, Chem. Phys. Lett. **83**, 1 (1981).
[15] S. W. Sharpe, R. Sheeks, C. Wittig, and R. A. Beaudet, Chem. Phys. Lett. **151**, 267 (1988).
[16] T. A. Hu, E. L. Chappell, and S. W. Sharpe, J. Chem. Phys. **98**, 6162 (1993).
[17] G. A. Blake, K. B. Laughlin, R. C. Cohen, K. L. Busarow, D.-H. Gwo, C. A. Schmuttenmaer, D. W. Steyert, and R. J. Saykally, Rev. Sci. Instrum. **62**, 1701 (1991).
[18] A. Van Orden, T. F. Giesen, R. A. Provencal, H. J. Hwang, and R. J. Saykally, J. Chem. Phys. **101**, 10237 (1994).
[19] K. Liu, M. G. Brown, J. D. Cruzan, and R. J. Saykally, Science **271**, 62 (1996).
[20] M. R. Viant, R. S. Fellers, R. P. McLaughlin, and R. J. Saykally, J. Chem. Phys. **103**, 5902 (1995).
[21] P. Horowitz and W. Hill, *The Art of Electronics* (Cambridge University Press, Cambridge, 1989).
[22] K. Liu, M. G. Brown, and R. J. Saykally (unpublished).
[23] K. Liu, J. G. Loeser, M. J. Elrod, B. C. Host, J. A. Rzepiela, N. Pugliano, and R. J. Saykally, J. Am. Chem. Soc. **116**, 3507 (1994).
[24] K. Liu, M. J. Elrod, J. G. Loeser, J. D. Cruzan, N. Pugliano, M. G. Brown, J. Rzepiela, and R. J. Saykally, Faraday Discuss. **97**, 35 (1994).
[25] J. D. Cruzan, L. B. Braley, K. Liu, M. G. Brown, J. G. Loeser, and R. J. Saykally, Science **271**, 59 (1996).
[26] K. Liu, M. G. Brown, and R. J. Saykally, Mol. Phys. (submitted).
[27] R. D. Brown, P. D. Godfrey, D. McNaughton, and A. P. Pierlot, J. Am. Chem. Soc. **110**, 2329 (1988).